

9.2 Boundary Layers

Contributed by:

C. Kähler, J. Kompenhans

The following two experiments have been performed in the DLR low turbulence wind tunnel (TUG), which is of an Eiffel type. Screens in the settling chamber and a high contraction ratio of 15:1 lead to a low turbulence level in the test section (cross section $0.3 \times 1.5 \text{ m}^2$). The basic turbulence level in the test section of the TUG of $Tu = 0.06\%$ (measured by means of a hot wire) allows the investigation of acoustically excited transition from laminar to turbulent flow as well as turbulent boundary layers that develop in the relatively long test section. The flow was seeded in the settling chamber upstream of the screens used to reduce the turbulence of the wind tunnel flow.

9.2.1 Boundary Layer Instabilities

In the case of periodic flows, the conditional sampling technique can be utilized in order to record instantaneous velocity vector maps always at the same phase angle. The excitation of the periodic process and the recording sequence must be phase locked. As an example for the application of conditional sampling, the investigation of instabilities in a boundary layer will be described.

The transitional process in a boundary layer is determined by a mechanism of generation and interaction of various instabilities. Small oscillations may cause primary instability – two-dimensional waves, the Tollmien-Schlichting (TS) waves. The growth of such TS waves leads to a streamwise periodic modulation of the basic flow, which gets sensitive to three-dimensional, spanwise periodic disturbances. These disturbances are amplified and lead to a three-dimensional distortion of the TS waves and farther downstream to the generation of three-dimensional Λ vortices. The extension of the knowledge about this mechanism enables the prediction and control of transition as required for applications in fluid mechanical engineering.

In order to study the behavior of instabilities, quantitative data of velocity fields with known initial conditions have been acquired in a flat plate boundary layer, in the TUG wind tunnel (see figure 9.7). In order to get reproducible and constant conditions for the development of the instabilities it is necessary to know the initial amplitude of the velocity fluctuations at the beginning of the observation area [276]. In the experiment of KÄHLER & WIEGEL this is achieved by introducing controlled disturbances by means of a device for acoustic excitation which consists of a single spanwise slot for the controlled input of two-dimensional disturbances and 40 separate slots (positioned

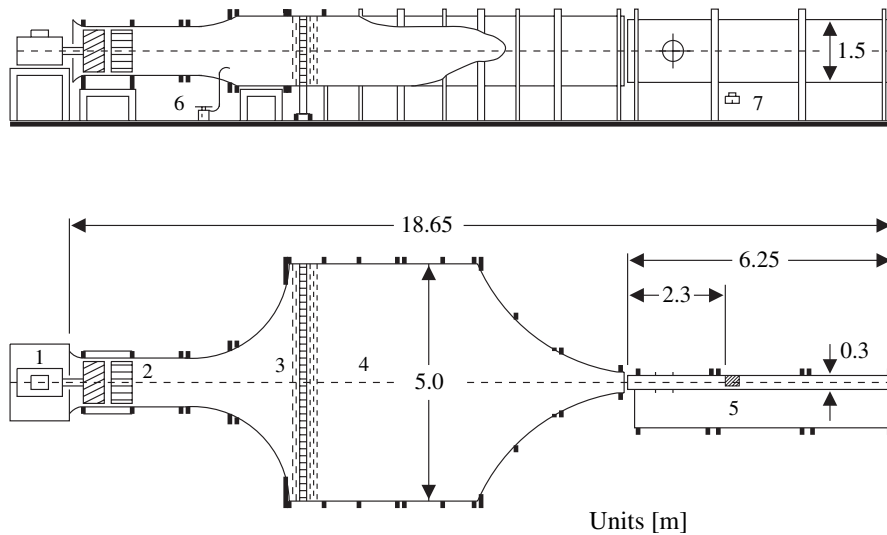


Fig. 9.7. Low turbulence wind tunnel.

Table 9.4. PIV recording parameters for boundary layer instabilities.

Flow geometry	parallel to light sheet and plate
Maximum in-plane velocity	$U_{\max} \approx 12 \text{ m/s}$
Field of view	$70 \times 70 \text{ mm}^2$
Interrogation volume	$1.9 \times 1.9 \times 0.5 \text{ mm}^3$ ($H \times W \times D$)
Dynamic spatial range	$\text{DSR} \approx 31 : 1$
Dynamic velocity range	$\text{DVR} \approx 137 : 1$
Observation distance	$Z_0 \approx 0.6 \text{ m}$
Recording method	dual frame/single exposure
Ambiguity removal	frame separation (frame-straddling)
Recording medium	full frame interline transfer CCD
Recording lens	$f = 60 \text{ mm}$, $f_{\#} = 2.8$
Illumination	Nd:YAG laser ^a 320 mJ/pulse
Pulse delay	$\Delta t = 80 \mu\text{s}$
Seeding material	oil droplets ($d_p \approx 1 \mu\text{m}$)

^a frequency doubled

spanwise as well) for the input of controlled three-dimensional disturbances. The velocity at the outer edge of the boundary layer was about $U = 12 \text{ m/s}$. The average free stream turbulence level was $Tu = 0.065\%$. The light sheet (thickness $\delta_Z = 0.5 \text{ mm}$ in the observation area) was oriented parallel to the plate. Its height above the plate could be varied but was usually 0.5 mm in the experiment. The observation area was $70 \times 70 \text{ mm}^2$. The PIV parameters used for this investigation are listed in table 9.4.

By applying different input signals to the acoustic excitation it was possible to excite different transition types. We mention here the *fundamental type*, the *subharmonic type* and the *oblique type*. Figure 9.8 presents the phase

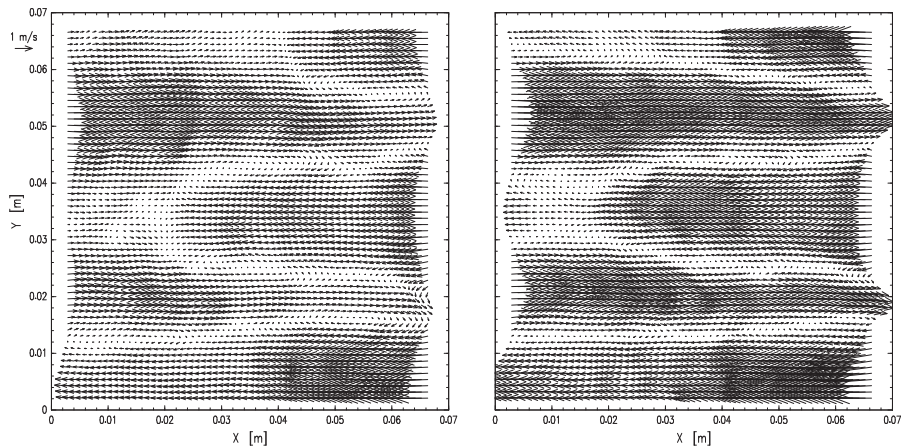


Fig. 9.8. Field of instantaneous velocity fluctuations of boundary layer instabilities above a flat plate for two different amplitudes of the input signal.

locked field of the instantaneous velocity fluctuations ($U - U_{\text{mean}}, V$) obtained by exciting the *oblique type* for two different disturbances. The Λ -vortices exhibit in an aligned pattern. The spanwise wavelength of these Λ -vortices (here ≈ 20 mm) matches with the wavelength of the controlled input of the 3D-waves.

The direction of the flow is from left to right. The mean velocity U_{mean} (calculated by averaging over all velocity vectors in the recording) has been subtracted from all velocity vectors in order to show the fluctuating components of the velocity vector field.

9.2.2 Turbulent Boundary Layer

The following PIV application in a turbulent boundary layer at the wall of a flat plate illustrates two problems: obtaining PIV data close to a wall and recovering PIV data even in a flow with gradients (due to the velocity profile of the boundary layer).

In the present series of experiments the measurement position was 2.3 m downstream of a tripping region in the low-turbulence wind tunnel (see figure 9.7) at the DLR-Göttingen research center [309]. At this position the turbulent boundary layer thickness δ was of the order of 5 cm, of which the lower 3 cm was imaged. At free stream velocities of 10.3, 14.9 and 19.8 m/s between 90 and 100 PIV image pairs were recorded. By removing a constant velocity profile of $U_{\text{ref}} = 8$ m/s from the PIV data set, the small scale struc-

Table 9.5. PIV recording parameters for turbulent boundary layer over a flat plate with zero pressure gradient.

Flow geometry	parallel to light sheet
Maximum in-plane velocity	$U_{\infty} = 10.3, 14.9, 19.8$ m/s
Field of view	30×30 mm ²
Interrogation volume	$2.0 \times 2.0 \times 1.0$ mm ³ ($H \times W \times D$) $2.0 \times 1.0 \times 1.0$ mm ³ ($H \times W \times D$) $2.0 \times 0.5 \times 1.0$ mm ³ ($H \times W \times D$) $1.0 \times 1.0 \times 1.0$ mm ³ ($H \times W \times D$)
Dynamic spatial range	DSR $\approx 31 : 1$
Dynamic velocity range	DVR $\approx 44 : 1$
Observation distance	$z_0 \approx 1.5$ m
Recording method	dual frame/single exposure
Ambiguity removal	frame separation (frame-straddling)
Recording medium	full frame interline transfer CCD
Recording lens	$f = 180$ mm, $f_{\#} = 2.8$
Illumination	Nd:YAG laser ^a , 70 mJ/pulse
Pulse delay	$\Delta t = 7 - 20$ μ s
Seeding material	oil droplets ($d_p \approx 1$ μ m)

^a frequency doubled

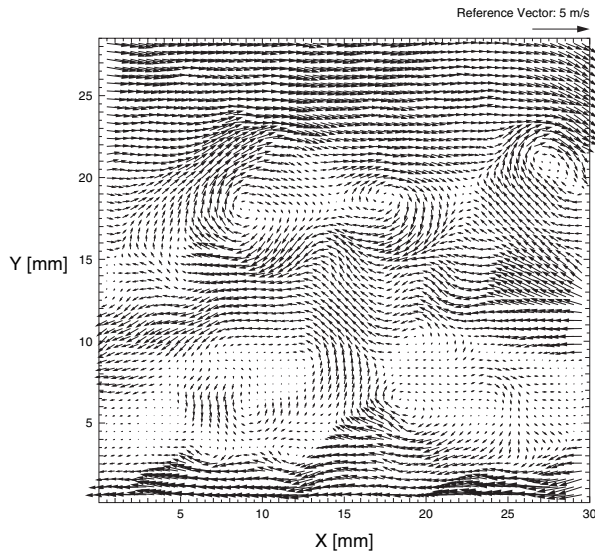


Fig. 9.9. Field of instantaneous velocity fluctuations in a fully turbulent boundary layer, $(U - U_{\text{ref}}, V)$. Position of the wall at $Y = 0$.

tures in the boundary layer are highlighted as can be seen in figure 9.9. It is remarkable how close to the wall, the velocity data could be recovered. The PIV parameters used for this investigation are listed in table 9.5.

In the first part of the evaluation the boundary layer profile and the RMS components of the velocity fluctuations were calculated as an average over all PIV recordings. These averaged quantities agree very well with the results from theory and pointwise velocity measurements as carried out by means of a hot wire. The nondimensional velocity profiles given in figure 9.10 start near the outer edge of the viscous sublayer ($y^+ \approx 10$) and extend well into the region where the large scale structures in the boundary layer cause a departure from the logarithmic profile ($y^+ \approx 200$).

As already mentioned, the strong velocity gradients within the interrogation areas close to the wall have mainly two effects.

First, due to the inhomogeneous displacement of paired particle images, the amplitude of the signal peak R_{D^+} is diminished. In addition, the diameter of the peak is broadened in the direction of shear. Therefore the velocity variation in the near wall region will decrease the likelihood of detection of the displacement peak.

Second, besides these experimental difficulties it has to be carefully checked whether the velocity vector assigned to the center of the interrogation window really represents the flow velocity at this location also in the presence of velocity gradients, as has been obtained by averaging over the interrogation window (see figure 6.15).

To investigate the effect of different interrogation area size on the number of outliers all PIV recordings were interrogated four times. The result can be

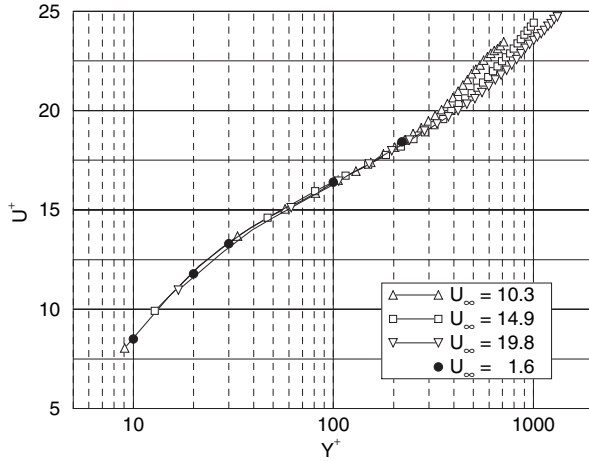


Fig. 9.10. Mean velocity profiles, scaled with inner variables (averaged over 100 PIV recordings).

seen in table 9.6 (for more details see [309]). The number of outliers in the 64×32 window is smaller compared to the other cases, because the number of particles is two times larger. The fraction of outliers is only of the order of 1% in the worst case, which clearly shows the reliability of the measurement technique.

Figure 9.11 represents the semilogarithmic mean velocity profiles as a function of the distance from the wall. For wall distances $y \geq 2$ mm the mean velocity is independent of the size of the interrogation window for three different measurements ($U_\infty = 10.3, 14.9$ and 19.8 m/s).

However, for $0 < y < 2$ mm the curves do not coincide due to the different averaging. The extension of the interrogation windows in the y direction is mainly responsible for this. Rectangular windows (extending parallel to the wall) show better performance as compared to square windows.

Windows deformation techniques for PIV evaluation as developed during the past few years have considerably contributed to the improvement of the data quality in boundary layers and shear flows. However, it should be stressed

Table 9.6. Number of outliers as a function of the interrogation area size, shape and free stream velocities.

$\Delta x_0 \times \Delta y_0$ [pixel]	outliers [%] [10.3 m/s]	outliers [%] [14.9 m/s]	outliers [%] [19.8 m/s]
32×32	1.07	1.00	1.26
64×16	0.72	0.58	1.03
64×32	0.20	0.21	0.30
64×64	0.14	0.19	0.17

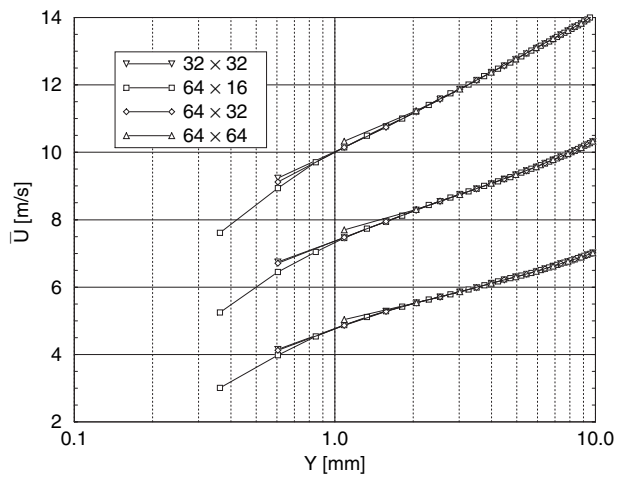


Fig. 9.11. Spatial resolution effects in the near wall region (averaged over 100 PIV recordings).

that a test on scale sensitivity (size and shape of interrogation window) of the velocity data and the number of outliers should be carried out in order to assess the data quality.